

Geometrically and chemically anisotropic particles at an oil-water interface

Supplementary Information

Bum Jun Park, Chang-Hyung Choi, Sung-Min Kang, Kwadwo E. Tettey, Chang-Soo Lee* and Daeyeon Lee*

Particle Preparation. To prepare Janus cylinders, we use a micromolding method described previously.¹ Briefly, for the apolar region, a mixture consisting of 900 μL of trimethylolpropane triacrylate, 100 μL of laury acrylate, 50 μL of Darocur 1173, and an appropriate amount of ethanol is introduced on the PDMS micromold with cylindrical wells, which are prepared by using soft lithography. Excess solution is removed by using a micropipette. Ethanol is allowed to evaporate and the solutions are exposed to UV (wavelength = 365 nm) for 2 min. Subsequently, a precursor mixture for the polar region, consisting of 700 μL of polyethylene glycol diacrylate ($M_n = 575$), 300 μL of pentaerythritol tetracrylate, and 50 μL of Darocur 1173 is added to the micromold, followed by UV irradiation for 2 min. The Janus cylinders formed in the PDMS micromold are recovered by suspending it in isopropyl alcohol. For a detailed description of the particle preparation, we refer the reader to Choi et al.¹ All chemicals are purchased from Sigma-Aldrich unless otherwise noted.

Pair Interaction Measurements. We use a particle tracking method to measure the interactions between two tilted Janus cylinders at a pure oil-water interface.² An image sequence is captured by a high speed camera (Phantom V7.1) at a frame rate of 300 frames/s. These digitized images are imported to ImageJ to track each particle position using the threshold algorithm.³ The particle separation (r) and the drift velocity (v) between the two attractive particles are computed from the obtained particle trajectories. The interaction force can be estimated by Stokes' drag force at a low Reynolds number limit ($N_{\text{Re}} = \frac{2Rv\rho}{\mu} \ll 1$, maximum

value of N_{Re} in the experiments is $\sim O(0.01)$) and is given by, $-F_{inter} = F_{drag} = \frac{1}{2} C_D \rho v L N_{Re}$.^{4,5} L and R are the length and diameter of the cylinder, ρ and μ is the density and viscosity of the fluid, respectively. The viscosity is approximated using the relative contact area of the particle to each liquid phase,⁶ $\mu_{eff} = (\mu_o \sqrt{S_r} + \mu_w \sqrt{1-S_r}) / (\sqrt{S_r} + \sqrt{1-S_r})$, where $S_r = S_{oil} / S_{tot}$ is the fraction of particle surface in contact with the oil phase. μ_o and μ_w are the viscosities of oil and water, respectively. The drag coefficient (C_D) can be numerically calculated at moderate Reynold numbers ($1 < N_{Re} < 40$) as a function of N_{Re} , AR , and the interparticle alignment,⁵ which is also valid at lower N_{Re} . The small in-plane rotation of the two particles observed in Fig. 3(a) during the assembly process does not significantly change the value of C_D in the range of experimental N_{Re} .⁵ Therefore, we determine the interaction force based on the assumption that the two particles are parallel to each other (Fig. 3(b)). Moreover, the small difference in the viscosities of the two fluid phases (i.e., $\mu_w = 0.001$ and $\mu_o = 0.00092$ Pa·s) unlikely influences the measured interaction force and also does not induce torque to rotate the particles out of the plane of the interface during their lateral movement. The largest potential that could induce rotation of an interface-trapped cylinder due to the viscosity difference is only about $O(10^5)k_B T$, which is negligible compared to the energy required to rotate a Janus cylinder by one degree, $\Delta E/d\theta_r \sim O(10^8)k_B T/\text{deg}$. Moreover, the lift force caused by the lateral translation of a tilted cylinder is not expected to displace the particle in the vertical direction. For instance, the ratio of lift-to-drag coefficients of a cylinder with $AR = 2.4$ with the rotation angle of $\theta_r = 50^\circ$ is about 0.08 at $N_{Re} = 0.01$.⁵ Assuming the drag coefficient of $C_D \sim O(10^3)$ in the experiments, the lift coefficient is $\sim O(10^2)$ and the resulting potential is $O(10^5)k_B T$, which is significantly smaller than the energy required to vertically displace the cylinder by 1% of its length, which is approximately $O(10^7)k_B T$.

Contact Angle. We prepare thin polymer films on glass slides by photopolymerizing each solution mixture consisting of apolar and polar parts. For the contact angle of the apolar polymer film, a water droplet is

gently placed on the apolar film in decane environment. The resulting contact angle is $\theta_A = 134 \pm 9^\circ$. For the polar polymer film, the inverted method is used; that is, a decane droplet is formed on the upside-down film in the aqueous phase. The measured contact angle is $\theta_P = 62 \pm 3^\circ$.

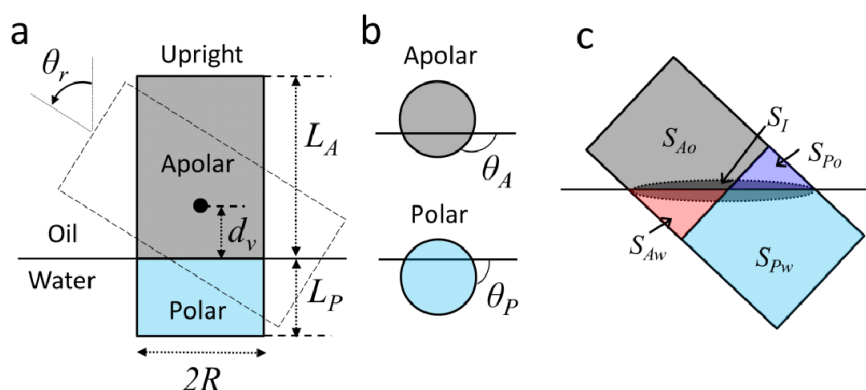


Fig. S1 Schematics for calculating the attachment energy of a Janus cylinder to the oil-water interface. (a) Janus cylinder consisting of apolar and polar surfaces. Black dot indicates the center-of-mass. θ_r and d_v show the orientation angle and the vertical displacement, respectively. (b) Three-phase contact angles of apolar (θ_A) and polar (θ_P) spheres at the interface. (c) A tilted orientation with polar and apolar surfaces in contact with the oil and water phases. The shaded region denotes the displaced area (S_I) of the interface due to the presence of the particle.

Attachment Energy Calculation. The orientation angle (θ_r) is defined as a tilt angle from the upright orientation (Fig. S1(a)); that is, the angle between the axes in the upright and a tilted orientation. The vertical displacement of the center-of-mass of the cylinder from the interface is denoted as d_v , which can alternatively be expressed by the fraction of particle surface in contact with the oil phase, S_{oil}/S_{tot} . The surface wettability of apolar and polar regions is characterized by the three-phase contact angles of homogenous apolar (θ_A) and polar (θ_P) spheres at the oil-water interface, respectively (Fig. S1(b)). The attachment energy of a Janus particle from water or oil to the planar oil-water interface is given by,^{7,8}

$$E_{Iw} = \gamma_{ow}(S_{Ao} \cos \theta_A + S_{Po} \cos \theta_P - S_I) \quad \text{from water} \quad (\text{S1})$$

$$E_{Io} = -\gamma_{ow}(S_{Aw} \cos \theta_A + S_{Pw} \cos \theta_P + S_I) \quad \text{from oil} \quad (\text{S2})$$

where γ_{ow} is the interfacial tension between oil and water ($\gamma_{ow} = 50$ mN/m for the decane-water interface). S_{ij} indicates the apolar ($i = A$) or polar ($i = P$) surface area in contact with water ($j = w$) or oil ($j = o$), as shown in Fig. S1(c). S_I is the displaced area of the oil-water interface due to the presence of the particle. The attachment energy is numerically calculated as a function of orientation angles (θ_r) and vertical positions (d_v), assuming that the interface remains flat. Our prior studies have shown that the effect of interface deformation around the particles on the equilibrium configuration of non-spherical amphiphilic particles is negligible.^{7,8} More importantly, this study shows that our calculations accurately predict the experimentally observed configuration of amphiphilic cylinders. Subsequently, the equilibrium configuration is determined by finding θ_r and d_v that minimize the attachment energy. This attachment energy of Janus cylinders is normalized by the surface area (S_0) of a cylinder with $AR = 1$ and $L = 10$ μm , $\Delta E(nor) = \Delta E \times (S_0 / S_{tot})$. This normalization enables us to study the effect of aspect ratio on the configuration of these cylinders while decoupling the effect of surface area. Note that the equilibrium configurations obtained from either Eqs. (S1) or (S2) result in the same configuration.^{7,8} Unless otherwise noted, we use Eq. (S1).

Surface Area Calculation. To calculate the surface area of a Janus cylinder exposed to each fluid phase (S_{ij} in Fig. S1(c)), we use the hit-and-miss Monte Carlo method.^{7,8} A Janus cylinder is generated by a large number of points (N_{tot}), which are homogeneously distributed on the surface. The value of S_{ij} is calculated by the product of the number fraction of the points ($P_{ij} = N_{ij}/N_{tot}$) and the total surface area ($S_{tot} = 2\pi R(R + L)$) and thus, is given by $S_{ij} = P_{ij} \cdot S_{tot}$. In this calculation, we assume that the three-phase contact line is smooth and flat. The effect of thermal fluctuation and gravity is negligible for particles that we consider in this study (i.e., Bond number, the ratio of gravitational force to surface tension force, is $Bo = \rho g R^2 / \gamma_{ow} \sim 10^{-4}$).

Quadrupolar or higher order interface deformation around a particle unlikely induces a torque to rotate the particle due to its symmetry. It also has been reported that the effect of asymmetric character on the deformation (i.e., dipole) probably caused by the preferred wetting (i.e., apolar surface by the oil phase and polar surface by the aqueous phase) can be neglected for the determination of equilibrium or metastable configurations.^{7,8}

Equilibrium Configuration. We use Eq. (S1) to calculate the attachment energy as a function of the orientation angle (θ_r) as well as the vertical displacement (d_v). For given parameters, such as θ_A/θ_P , L_A/L_P , and AR , we scan the attachment energy ($\Delta E(d_v, \theta_r = \Theta)$) by varying d_v at a constant value of $\theta_r = \Theta$. The minimum attachment energy at this particular orientation angle of $\theta_r = \Theta$ is given by $\Delta E_{min}(\theta_r = \Theta)$ where $d_v = d_{v,min}$. Using the same procedure, ΔE_{min} 's are readily obtained as a function of θ_r ranging from 0° to 90° with the increment of 1° . The global (or equilibrium) energy minimum (ΔE_{eq}) is found as the lowest one among the obtained values of ΔE_{min} (i.e., $\Delta E_{eq} = \min(\Delta E_{min})$). The corresponding equilibrium orientation and vertical displacement at this global energy minimum are $\theta_{r,eq}$ and $d_{v,eq}$, respectively.

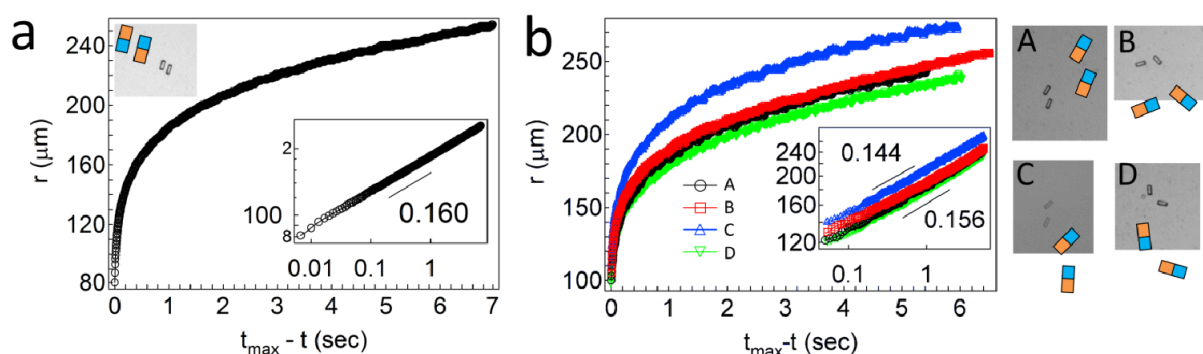


Fig. S2 Center-to-center separation, r , versus $(t_{\max} - t)$ when two tilted Janus cylinders with $AR = 2.4^S$ approach in the side-to-side direction (a) and in other alignments (b). Insets in each panel are the corresponding log-log plot. Snapshots

and schematics indicate the alignments of the particles before they come in contact at $t = t_{max}$. The power law exponent in the inset of panel (b) is fitted as $\alpha = 0.156$ (A), 0.154 (B), 0.147 (C), and 0.144 (D) with a fitting error of $O(10^{-3}) - O(10^{-4})$.

Pair Interactions for $AR = 2.4^S$. The pair interactions between tilted Janus cylinders with $AR = 2.4^S$ at the oil-water interface are also measured. Consistent with the results of $AR = 2.4^A$ in Fig. 3, the power law exponent when two particles approach side-to-side is obtained as $\alpha \approx 0.16$, suggesting that the interaction is dominated by the quadrupolar interaction (Fig. S2(a)). When the particles approach while the polar end surface of at least one particle aligns itself toward the other particle, the value of α varies in the range of 0.144-0.156 (Fig. S2(b)). This result indicates the possible contribution of higher order interface deformation such as hexapoles.

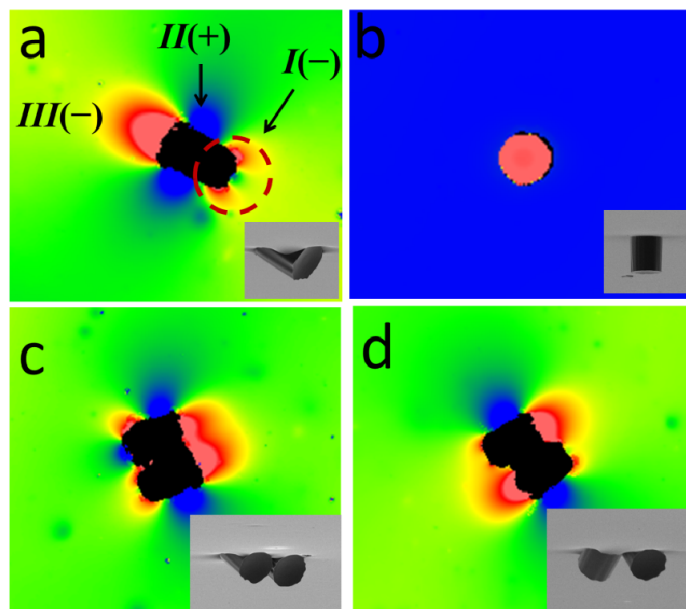


Fig. S3 Profilometry images of interface deformation around (a) a tilted Janus cylinder ($AR = 2.4^S$), (b) upright-oriented cylinder, (c and d) two attached cylinders side-by-side with orientation angles of each particle, (c) $\theta_{r,1} \approx \theta_{r,2}$

and (d) $\theta_{r,1} \approx -\theta_{r,2}$. The particles are partially embedded in a PDMS slab (inset SEM images) prepared by using the gel trapping method.

Interface Deformation for $AR = 2.4^S$. The quasi-quadrupolar interface deformation (Fig. S3(a)) around the particles with $AR = 2.4^S$ accounts for the obtained scaling behaviors which depend on the interparticle alignments. Similar to the case of $AR = 2.4^A$ in Fig. 4, the net negative interface meniscus around the polar end surface imparts a hexapole-like character to the measured interaction between two tilted particles when they are aligned arbitrarily, rather than side-to-side (Figs. S3(b) and S3(c)). The interface deformation around a cylinder with the upright orientation is negligible due to the pinned WSL at the oil-water interface (Fig. S3(b)), resulting in negligible capillary interactions between them.

Reference

1. C.-H. Choi, J. Lee, K. Yoon, A. Tripathi, H. A. Stone, D. A. Weitz and C.-S. Lee, *Angew. Chem. Int. Edit.*, 2010, **49**, 7748-7752.
2. J. C. Loudet, A. M. Alsayed, J. Zhang and A. G. Yodh, *Phys. Rev. Lett.*, 2005, **94**, 018301-018304.
3. C. A. Schneider, W. S. Rasband and K. W. Eliceiri, *Nat. Meth.*, 2012, **9**, 671-675.
4. K. O. L. F. Jayaweera and B. J. Mason, *J. Fluid Mech.*, 1965, **22**, 709-720.
5. A. Vakil and S. I. Green, *Comput. Fluids*, 2009, **38**, 1771-1781.
6. B. J. Park, J. P. Pantina, E. M. Furst, M. Oettel, S. Reynaert and J. Vermant, *Langmuir*, 2008, **24**, 1686-1694.
7. B. J. Park and D. Lee, *ACS Nano*, 2012, **6**, 782-790.
8. B. J. Park and D. Lee, *Soft Matter*, 2012, **8**, 7690-7698.